REPORT DOCUMENTATION PAGE	Form Approved OMB No. 0704-0188

PLEASE DO NOT RETURN YOUR FORM TO THE ABOVE ORGANIZATION.

1. REPORT DATE (DD-MM-YYYY)	2. REPORT TYPE	3. DATES COVERED (From - To)
02-03-2011	Conference Proceeding	

4. TITLE AND SUBTITLE

Intercomparison of Atmospheric Correction Algorithms Applied to HICO Imagery

5a. CONTRACT NUMBER

5b. GRANT NUMBER

5c. PROGRAM ELEMENT NUMBER

0602435N

6. AUTHOR(S)

Ruhul Amin, Richard Gould, Weilin Hou, Paul Martinolich, Marcos Montes and Robert Arnone

5d. PROJECT NUMBER

5e. TASK NUMBER

5f. WORK UNIT NUMBER

73-6287-A0-5

7. PERFORMING ORGANIZATION NAME(S) AND ADDRESS(ES)

Naval Research Laboratory
Oceanography Division
Stennis Space Center, MS 39529-5004

8. PERFORMING ORGANIZATION REPORT NUMBER

NRL/PP/7330--10-0412

9. SPONSORING/MONITORING AGENCY NAME(S) AND ADDRESS(ES)

Office of Naval Research
800 N. Quincy St.
Arlington, VA 22217-5660

10. SPONSOR/MONITOR'S ACRONYM(S)

ONR

11. SPONSOR/MONITOR'S REPORT NUMBER(S)

12. DISTRIBUTION/AVAILABILITY STATEMENT

Approved for public release, distribution is unlimited.

13. SUPPLEMENTARY NOTES

14. ABSTRACT

In this study we examine results from two atmospheric correction approaches applied to HICO data. The first atmospheric correction approach is the standard multispectral Gordon/Wang NIR atmospheric correction applied to HICO MODIS-like channels using appropriate MODIS relative spectral response tables. The second approach is the Cloud and Shadow (C&S) atmospheric correction which is a scene-dependent method that requires accurate detection of a cloud-shadow pair and a neighboring sunny region which has the same water properties as the shadow region. Although clouds are relatively easy to detect, detecting their shadows over deep water is quite challenging. In this study we also introduce an automated cloud shadow detection approach; for convenience we call it the Cloud Shadow Algorithm (CSA) and it seems to work reasonably well over homogeneous water bodies. We present some preliminary results comparing the two atmospheric correction approaches and also some preliminary results of the shadow detection approach.

15. SUBJECT TERMS

atmospheric correction, HICO, cloud shadow algorithm, automated, homogeneous water bodies

16. SECURITY CLASSIFICATION OF:			17. LIMITATION OF ABSTRACT	18. NUMBER OF PAGES	19a. NAME OF RESPONSIBLE PERSON
a. REPORT	b. ABSTRACT	c. THIS PAGE			Richard Gould
Unclassified	Unclassified	Unclassified	UL	7	19b. TELEPHONE NUMBER (Include area code) 228-688-5587

Intercomparison of Atmospheric Correction Algorithms Applied to HICO Imagery

Ruhul Amin[1], Richard W. Gould[1], Weilin Hou[1], Paul Martinolich[1], Marcos J. Montes[2], and Robert A. Arnone[1]
[1]Naval Research Laboratory, Code 7333, Stennis Space Center, Mississippi 39529, USA
[2]Naval Research Laboratory, Code 7212, Washington, DC, 20375, USA

The Hyperspectral Imager for the Coastal Ocean (HICO) has been operating on board the International Space Station since installation on 24 September 2009. HICO provides 100 m resolution hyperspectral imagery optimized for the coastal ocean. However, accurate retrieval of bio-optical properties from these ocean color measurements relies on accurate atmospheric corrections; a small inaccuracy in atmospheric corrections can lead to significant errors in the retrieved products.

In this study we examine results from two atmospheric correction approaches applied to HICO data. The first atmospheric correction approach is the standard multispectral Gordon/Wang NIR atmospheric correction applied to HICO MODIS-like channels using appropriate MODIS relative spectral response tables. The second approach is the Cloud and Shadow (C&S) atmospheric correction which is a scene-dependent method that requires accurate detection of a cloud-shadow pair and a neighboring sunny region which has the same water properties as the shadow region. Although clouds are relatively easy to detect, detecting their shadows over deep water is quite challenging. In this study we also introduce an automated cloud shadow detection approach; for convenience we call it the Cloud Shadow Algorithm (CSA) and it seems to work reasonably well over homogeneous water bodies. We present some preliminary results comparing the two atmospheric correction approaches and also some preliminary results of the shadow detection approach.

INTRODUCTION

The fundamental measurement in ocean color remote sensing is the water-leaving radiance, the upwelling spectral distribution of the radiance from the ocean. Geophysical parameters such as chlorophyll concentrations can be retrieved from this water-leaving signal since it contains information about the optically-active components in the water column. However, only about 10% of the total signal measured by the ocean color sensors contains information about the waters; the rest represents scattering from aerosols and air molecules. The goal of the atmospheric correction over the ocean is to remove contributions from the atmosphere and reflection from the sea surface.

Gordon and Wang (1994) [1] developed an atmospheric correction scheme for the open ocean where the aerosol contribution is estimated using Top of the Atmosphere (TOA) radiance/reflectance signals obtained from near infrared (NIR) bands. This approach assumes that the ocean is optically black in the NIR bands due to the strong water absorption. Although this technique works well in the open ocean, it breaks down in optically complex coastal waters, since the black pixel approximation no longer holds true due to strong reflections from organic and inorganic particulate matters. If water-leaving radiance is not negligible in the NIR bands then the retrieved aerosol loading will be overestimated, resulting in underestimated or even negative water-leaving radiances. However, for our data processing we use the NIR-iterative procedure for the coastal waters [2] and standard NIR procedure for open ocean on multispectral (convolved) HICO MODIS-like bands. The NIR-iterative procedure reduces number of pixels with negative readings in the coastal waters. Another atmospheric

correction approach for coastal water was proposed [3] which uses short wave infrared (SWIR) bands. This approach is based on the fact that ocean water absorbs strongly in this spectral region, and the contributions of the in-water constituents are negligible and can safely be considered dark. However, these SWIR bands don't exist on Hyperspectral Imager for the Coastal Ocean (HICO). Furthermore, the atmospheric reflectance itself is significantly weaker in SWIR region and spectral features are particularly difficult to resolve. In such situations, the cloud and shadow (C&S) atmospheric corrections [4, 5] can be very helpful. However, C&S is limited to images with cloud and shadow present.

The C&S atmospheric correction method [4, 5] is appropriate for high-spatial resolution sensors such as HICO. This approach uses cloud and shadow pixels along with close by sunny pixels with similar optical properties. First, it estimates the atmospheric and sea-surface reflectance La from a pair of adjacent pixels that are in and out of a cloud shadow while ignoring the slight (<5%) differences in the remote-sensing reflectance $R_{rs}(\lambda)$ under the two regions [6-9]. Estimation of La also requires an estimate of the ratio between the downwelling sky irradiance to total downwelling irradiance $E_d^{sky}(\lambda)/E_d(\lambda)$ which can be estimated using Radtran [10] for a given location and time. In order to calculate $R_{rs}(\lambda)$, the product of atmospheric transmittance and downwelling irradiance $t(\lambda)E_d(\lambda)$ just above the surface is also needed. For this component the radiance over the cloud is used to make the estimate. Once the $R_{rs}(\lambda)$ is estimated to account for any residual contributions from the sky and sea surface, a spectrally constant value is removed from the calculated $R_{rs}(\lambda)$ in order to obtain an average of zero for the spectral range of 810-840 nm, where contributions from water are considered null [11].

In this study we compare HICO data atmospherically corrected using the standard NIR and C&S methods for a scene over Key Largo, Florida taken on November 13, 2009. Furthermore, we also introduce a cloud shadow detection approach called Cloud Shadow Algorithm (CSA) and present some preliminary results using HICO data.

THEORETICAL BACKGROUND AND DEVELOPMENT OF THE CLOUD SHADOW ALGORITHM

Identification of cloud shadows over water still remains a challenge from space borne visible sensors. It is very difficult to distinguish the water bodies from the shadow areas if it is based on spectral reflectance shape and amplitude information [12]. However, accurate identification of shadows is very important, because optical properties retrieved from these pixels will be in error. Additionally, they can be used with their cloud pair and adjacent sunny region to remove the atmospheric interference, which still remains a challenge particularly over turbid coastal waters.

Assume a small, compact, thick cloud over water removes direct solar photons and shadows a region. The water-leaving radiance from the shadowed region, $Lw_{sdw}(\lambda)$ that reaches the sensor results from only skylight photons since direct photons are removed by the cloud. An adjacent patch of water from a sunny region has identical inherent optical properties to those of the shadow region. Refer water-leaving radiance from the neighboring sunny region as $Lw_{sny}(\lambda)$, which results from illumination of both direct solar and skylight photons.

In addition to the water-leaving radiance, radiance recorded at the sensor also includes path radiance due to molecular (or Rayleigh) scattering and particulate (or aerosol) scattering from the field of view of the sensor. The path radiance can be due to only Rayleigh scattering, only aerosol scattering, or some combination of both. These three types of path radianee are denoted by L_r, L_a and L_{ra} respectively.

The total radiance measured at the sensor's altitude from the sunny area can be expressed as

$$Lt_{sny}(\lambda) = L_r(\lambda) + L_a(\lambda) + L_{ra}(\lambda) + t(\lambda)Lw_{sny}(\lambda) \tag{1}$$

where $t(\lambda)$ represents the diffuse transmittance of the atmosphere for the water-leaving radiance.

The total radiance measured at the sensor's altitude over the shadowed region can be expressed similarly, but some differenees in the path radiance and diffuse transmittance can be expected. The path radiance from the shadow region should be lower since part of the viewing path to the shadowed region is also shadowed, so it must produce less path radianee depending on how much of the atmosphere is shadowed [5]. While the apparent path transmittance of the water-leaving radiance from the shadowed region maybe slightly higher sinee the adjaeent areas of the scene are generally brighter and so the apparent transmittance of the viewing path to the shadow will be enhanced by photons reflected from the bright portion of the image and scattered into the field of view of the sensor [5].

So the total radianee measured over the shadowed region can be expressed as

$$Lt_{sdw}(\lambda) = L_r(\lambda) - \Delta L_r(\lambda) + L_a(\lambda) - \Delta L_a(\lambda) + L_{ra}(\lambda) - \Delta L_{ra}(\lambda) + (t(\lambda) + \Delta t(\lambda))Lw_{sdw}(\lambda) \tag{2}$$

The Δ term represents the perturbations due to the differences in scene illumination from the sunny pixels.

The water-leaving radiance can be expressed as two parts: one part caused by the backscattering of the diffuse skylight and the other part by backscattering of the direct solar beam. For the sunny and shadow region, it can be expressed as

$Lw_{sny}(\lambda) = Lw_{sny}^{sky}(\lambda) + Lw_{sny}^{dir}(\lambda)$ and $Lw_{sdw}(\lambda) = Lw_{sdw}^{sky}(\lambda)$ respectively

Because $Lw_{sdw}^{dir}(\lambda) = 0$

Where $Lw_{sny}^{sky}(\lambda)$ and $Lw_{sny}^{dir}(\lambda)$ represents water-leaving radiance caused by diffuse skylight and direct solar beam in the sunny region respectively, while $Lw_{sdw}^{sky}(\lambda)$ and $Lw_{sdw}^{dir}(\lambda)$ represents water-leaving radiance caused by diffuse skylight and direct solar beam in the shadow region respectively.

The diffuse irradiance incident on the shadow and close by sunny areas are unequal because scattering from cloud may increase the diffuse irradianee incident at the neighboring sunny region [5]. So, according to Reinersman et al., 1998 $Lw_{sny}^{sky}(\lambda)$ can be expressed as $Lw_{sny}^{sky}(\lambda) = Lw_{sdw}^{sky}(\lambda) + \Delta Lw_{sdw}^{sky}(\lambda)$.

Based on the above hypothesis, it can be expected that the water-leaving radiance from the shadow region ($Lw_{sdw}(\lambda)$) reaching the satellite sensor is lower than the water-leaving radiance from the neighboring sunny region ($Lw_{sny}(\lambda)$). But, we are assuming that the optical properties in the two regions are the same (because they are adjacent). Also the total path radiance from the shadow region is slightly lower since part of the atmosphere is also shadowed which must produce less path radiance depending on how much of the atmosphere is shadowed. As a result the total radiance measured over the shadowed region is lower than the neighboring sunny region. Even though these differences are small, we find that integrating the blue-green region of the spectrum amplifies these small differences and allows separation of the two regions. However, integration alone is not adequate to separate them using a threshold. To achieve separation, we normalize the integrated value (IV) of the pixel under question (needs to be classified either as a shadowed or sunny pixel), by the mean of the IV values within an Adaptive Sliding Box (ASB) centered on this pixel.

We define our cloud shadow detection approach based on the water and atmospheric characteristics of shadow and neighboring sunny region. For convenience, we call this the Cloud Shadow Algorithm (CSA):

$$IV = \int_{Blue}^{Green} Lt(\lambda)d\lambda \tag{3}$$

$$CSA = \frac{IV(\odot)}{mean(IV(\square))} \tag{4}$$

Where $IV(\odot)$ represents the IV value at the pixel which need to be classified either as a shadow or sunny pixel. The ASB should be selected centered on this pixel. The $mean(IV(\square))$ represents the mean of IV values within the selected ASB of this pixel. This process should be repeated for all pixels except for the edge pixels. The edge pixels are ignored for now since an ASB cannot be selected centered on these pixels. For this study we selected a constant 32×32 pixel ASB. Note that before applying CSA, land and clouds should be masked otherwise spurious results can be expected.

Our preliminary study on 16 selected HICO images shows that $CSA < 0.96$ seem to separate the shadowed pixels reasonably well. This is because the ASB for any particular pixel have only sunny and/or shadow pixels (everything else should be removed) and the water is homogeneous within the ASB. So, for a shadow pixel the CSA will shrink since the IV value (numerator of eq. 4) will be smaller than the mean of the ASB (denominator of eq. 4) which has both shadow and sunny pixels. While for a sunny pixel the CSA will be around one if ASB has only sunny pixel and greater than one if ASB has both sunny and shadow pixels. So, the proposed threshold can separate them easily. However, if the ASB contains only shadow pixels, this will create problems. So, the ASB need to be selected carefully so that it is slightly larger than the shadow size, which can be approximated using cloud size information that is relatively easy to determine. Also if the water is non-homogeneous within the ASB, spurious results can be expected. Thus, CSA should be appropriate for homogeneous water bodies such as open ocean. However, an observer can use the IV values (eq. 3) to visually identify the clouds and shadows over non-homogeneous waters.

RESULTS AND DISCUSSIONS

The CSA shadow detection approach with the proposed threshold has been tested on 16 HICO images and the results were compared visually with the true color images. Our preliminary result shows that CSA in general detects cloud shadows reasonably well over homogeneous water bodies. Figure 1 is an example of shadow detection over Virgin Island collected on December 20, 2009. Since most of our tested images have small puffy cumulus clouds, we used a constant 32×32 ASB box to determine CSA values. However, to detect all size of shadows the ASB should be selected carefully so that it doesn't only contain shadow pixels.

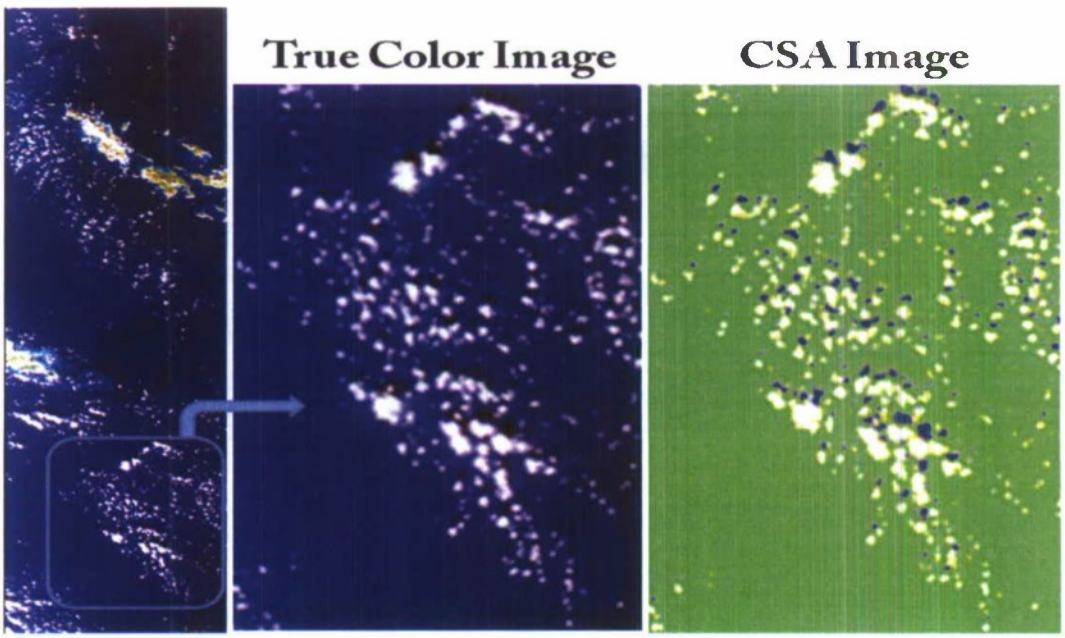

Figure 1. HICO Image acquired over Virgin Island on December 20, 2009. Left: full scene true color image; centre: zoomed view of true color image; right: zoomed view of CSA image.

Figure 2 shows $R_{rs}(\lambda)$ from the coastal waters of Key Largo, Florida collected on November 13, 2009. Solid lines are $R_{rs}(\lambda)$ calculated using the C&S atmospheric correction while the dashed lines with squares are $R_{rs}(\lambda)$ calculated using standard NIR atmospheric correction at HICO MODIS-like channels. These spectra are averaged over 2×2 pixels. The spectra with the same color (solid and dashed) in the right panel of Fig. 2 are taken from the same location, which is indicated in the left panel of Fig. 2 with the same colored squares. In general, both atmospheric corrections seem to agree in these coastal waters. However, MODIS-like spectra seem to have some problem at the 412nm channel where significantly higher values are observed. We are still investigating this issue. On the other hand, the C&S spectra seem reasonable, and typical of coastal areas. Unfortunately, no in-situ data is available to validate the results.

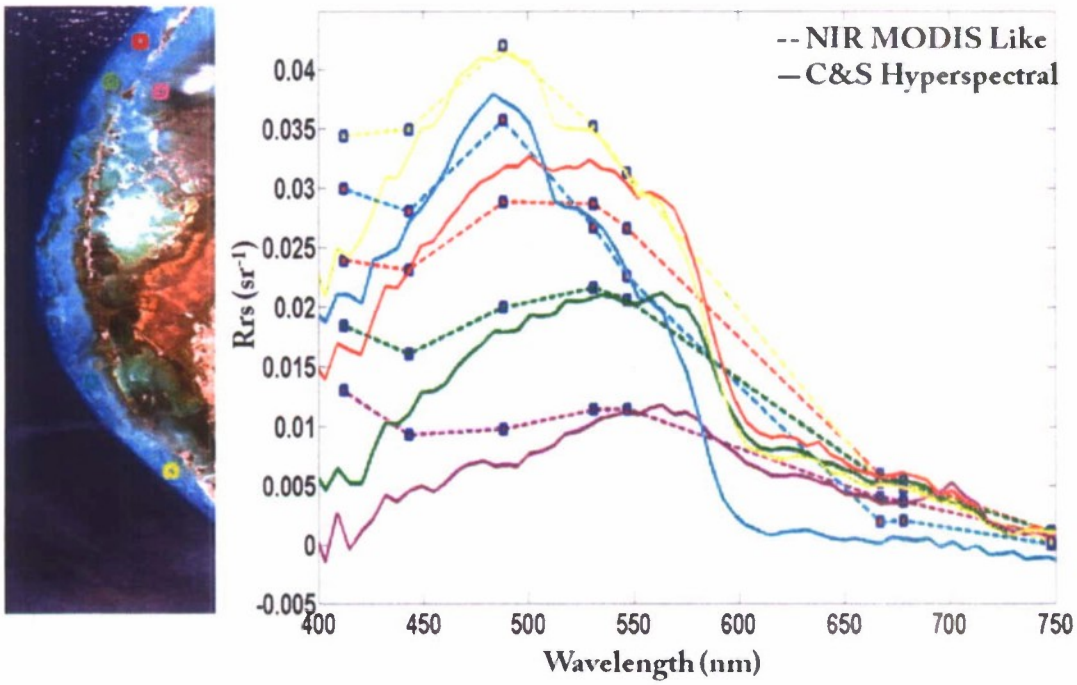

Figure 2. Left: HICO true color image (November 13, 2009) over Florida, Key Largo. Right: Remote-sensing reflectance spectra from the pixels indicated in the left scene. Solid lines are $R_{rs}(\lambda)$ corrected using C&S method and dashed lines with squares are $R_{rs}(\lambda)$ corrected using standard NIR method at HICO MODIS like channels. Solid and dashed spectrums with same color represent same location which is indicated in left scene with same color square box and they are averaged over 2×2 pixels.

CONCLUSION

Our preliminary results on HICO data show that the CSA cloud shadow detection approach seems to work reasonably well over Open Ocean. However, further studies are required to fully automate the approach, in particular how to select the ASB for any particular pixel and how to account for edge pixels (which are currently being ignored).

The Cloud and Shadow atmospheric correction yields reasonable reflectance values. However, additional work is required to validate the results using in situ data. The NIR atmospheric correction applied to the multispectral (convolved) HICO bands yields reasonable results over coastal areas. Issues with the 412nm channel are under investigation. In addition, we are developing a hyperspectral NIR approach that is under evaluation.

ACKNOWLEDGEMENTS

NRL Program Element PE0602435N Realizing the Naval Scientific Return of HICO

REFERENCES

1. H. R. Gordon, and M. Wang, "Retrieval of water-leaving radianee and aerosol optieal thiekness over the oeeans with SeaWiFS: a preliminary algorithm," Appl. Opt. **33**, 443-452 (1994)

2. R. P. Stumpf, R. A. Arnone, R. W. Gould, P. M. Martinolich, V. Ransibrahmanakul, "A partially coupled oeean-atmosphere model for retrieval of water-leaving radianee from SeaWiFS in coastal waters," *SeaWiFS postlaunch technical report series, Vol. 22*, S. B. Hooker and E. R. Firestone, Eds., *NASA/TM-2003-206892, (2003)*

3. M. Wang, and W. Shi, "Estimation of oeean eontribution at MODIS near infrared wavelengths along the east coast of the U.S.: two ease studies," Geophys. Res. Lett. **32**, L13606, doi: 10.1029/2005GL022917, (2005)

4. Z. P. Lee, B. Casey, R. Arnone, A. Weidemann, R. Parsons, M. J. Montes, B. Gao, W. Goode, C. O. Davis, J. Dye, "Water and bottom properties of a eoastal environment derived from Hyperion data measured from the EO-1 spaeecraft platform," Journal of Appl. Remote Sensing, Vol. 1, 011502 (2007)

5. P. Reinersman, K. L. Carder, and F. R. Chen, "Satellite-sensor ealibration verifieation with the cloud-shadow method," Appl. Opt. **37**, 5541-5549 (1998)

6. Z. P. Lee, K. L. Carder, C. D. Mobley, R. G. Steward, and J. S. Pateh, "Hyperspeetral remote sensing for shallow waters. 1. A semianalytieal model," Appl. Opt. **37**, 6329-6338 (1998)

7. J. T. O. Kirk, "Volume seattering funetion, average eosines, and the underwater light field," Limnol. Oeeanogr. **36**, 455-467 (1991)

8. A. Morel and B. Gentili, "Diffuse reflectanee of oeeanie waters (2): Bi-direetional aspeets," Appl. Opt. **32**, 6864-6879 (1993)

9. Z. P. Lee, K. L. Carder, and K. P. Du, "Effeets of molecular and particle scattering on model parameters for remote-sensing refleetanee, "Appl. Opt. **43**, 4957-4964 (2004)

10. W. W. Gregg and K. L. Carder, "A simple speetral solar irradianee model for eloudless maritime atmospheres," Limnol., Oeeanogr, **35**, 1657-1675 (1990)

11. J. L. Mueller, C. Davis, R. Arnone, R. Frouin, K. L. Carder, Z. P. Lee, R. G. Steward, S. Hooker, C. D. Mobley, and S. McLean, " Above-water radianee and remote sensing reflectance measurement and analysis protoeols," *in Ocean Optics Protocols for Satellite Ocean Color Sensor Validation*, ***Revision 3***, J. L. Mueller and G. S. Fargion, Eds., *NASA/TM-2002-210004*, 171-182 (2002)

12. R. Richter and A. Muller, "De-shadowing of satellite/airborne imagery," International Journal of Remote Sensing, Vol. 26, No. 15, 3137-3148 (2005)